NIGHTTIME FLOW AND DISPERSION OVER LARGE BASINS OR MINING PITS

by

Robert N. Meroney[1]

Clive Grainger[2]

Prepared for Submission to

Symposium on Measurement and Modeling of Environmental Flows
1992 ASME Winter Annual Meeting
Anaheim, California--November 8-13, 1992

Fluid Mechanics and Wind Engineering Program
Civil Engineering Department
Colorado State University
Fort Collins, Colorado
80523

July 3, 1992

[1] *Department of Civil Engineering, Colorado State University, Colorado, USA*
[2] *Department of Mechanical Engineering, Monash University, Victoria, Australia*

CEP92-93RNM-CG-1

Table of Contents

NIGHTTIME FLOW AND DISPERSION OVER LARGE BASINS OR MINING PITS

by
Robert N. Meroney[1] and Clive Grainger[2]

[1] *Department of Civil Engineering, Colorado State University, CO, USA*
[2] *Department of Mechanical Engineering, Monash University, Victoria, Australia*

Abstract. Discharges from spontaneous combustion within a large open-pit coal mine which occur during nighttime inversion conditions may result in stagnant accumulation of smoke and dangerous gases which could inhibit mining operations. A wind-tunnel model study was performed to identify the range of flow and mixing conditions which could exist when stably stratified atmospheric surface flows pass over a large open pit or basin. A novel arrangements to create stratified flows in large wind tunnels using distributed electrical heaters and an inverted ground plane to simulate night time inversions was employed. Flow penetration into the basin depended upon approach flow stability (Froude number) and the strength of thermal inversion within the basin. Measurements of wind speed and temperature were made upwind, within, and downwind of the basin. Concentration measurements were made within the basin of surface sources released along basin walls. Pollutant levels were found to be strong functions of the approach flow basin Froude number, source location, and release time.

1. **INTRODUCTION**

A terrace mining system has been proposed by the Electricity Trust of South Australia (ETSA) to mine the Leigh Creek coal field in South Australia. Once a minimum amount of overburden is removed above a coal seam all subsequent earth movement would be made along terraces by horizontally transporting unwanted earth above the unmined coal seam and dumping it on top of previously mined land (See Figure 1). This technique minimizes vertical transport of overburden; thus decreasing truck transport costs. The terracing system also reduces disturbance of unmined lands, automatically restores the overburden to surface mined regions, and limits the environmental impact of an open-basin mine operation.

After the loose overburden is dumped on the trailing terraces, residual coal and oil shale contained within the earth will combine with moisture resulting in spontaneous combustion generating dangerous fumes and smoke which ooze out of the overburden. Thus pollution sources may exist at various heights along the basin side walls, producing fumes of negligible buoyancy. Unless these combustion products are ventilated critical pollutants will rise over safe working limits.

When stably stratified surface flows are combined with night-time radiation surface cooling of the coal pit, surface flows may uncouple from the cooler air pooled within the excavation resulting in zero ventilation and continuous buildup of combustion products in the coal pit. Thus, this study focuses on stably stratified atmospheric conditions which are expected to produce critical pollutant levels. First, related studies of valley flows, nocturnal drainage flows in mountain basins, and the nature of mixing across inversions are examined. Next, measurements of wind speed, temperatures and dispersion over a 1:600 scale model of a generic coal pit are obtained.

The stratified flows found over open-pit mines are expected to be similar to night-time drainage flows that develop over mountain basins due to accumulation of downslope cold air and nocturnal cooling. Most observations, analysis and research in this area have related to open-ended valleys of simple nocturnal slope winds where accumulation does not persist (Whiteman, 1990). The development of inversions above mountain basins begins in a similar manner to valley flows, but the inversion depth and strength tend to be stronger than those found over valleys or flat terrain (Maki *et al.,* 1986).

Typically, side wall drainage flow begins during early evening as the sun ceases to shine on one wall of the basin. This may well start a few hours earlier than the cooling at the bottom because of the topographic effect on the real sunset time. The cooler air accumulates at the bottom of the basin and joins air cooled through ground contact with soil which loses heat through radiation to the night sky. A still-calm layer develops to about 1/4 the depth of the valley, at which point the drainage flow begins to fill in on top of the pool of cold air (Maki and Harimaya, 1988; Whiteman, 1990).

Simulation of atmospheric motions by wind-tunnel flows has occurred for almost 100 years since Professor LeCour constructed a wind-mill test facility in Askov, Denmark, in 1895 and Gustaf Eifel designed his exhibition tower in 1889. Background reviews about laboratory simulation were prepared by Cermak (1975), Davenport and Isyumov (1967) and Melbourne (1977). Meroney (1981) considered the simulation of complex terrain and valley drainage situations. Snyder (1981) suggested similarity criteria for the study of air-pollution meteorology in near neutral situations. Meroney (1987) extended the discussion to the simulation of dense-gas plumes in the surface layer. Meroney et al. (1975) and Avissar et al. (1990) proposed simulation criteria and operating ranges for the simulation of sea and land breezes. Meroney (1990) provides an extended discussion of modeling limitations, similarity considerations, facilities, and insights obtained from specific studies of both neutral and stratified flow over complex terrain.

Physical modeling studies of atmospheric flow over hills and mountains span 60 years of research. Dependent upon stratification, hill geometry and spacing various combinations of waves, downslope winds, valley penetration, streamwise division, upwind penetration, and blocking can be reproduced in the laboratory (Meroney, 1990). Measurements of isothermal boundary layers passing over sinusoidal boundaries were reported by Beebe (1972). Valley drainage flow situations have previously been simulated in wind tunnels by Hertig (1986) and Cermak and Petersen (1981). Grainger and Meroney (1992) described inverted floor simulation of stably stratified flow over Australian open-pit coal mines as compared to numerical and linear perturbation models.

Flow visualization experiments using valley models towed through salt-water have been completed at the Division of Atmospheric Research, CSIRO, Aspendale, Australia. Experiments by Bell and Thompson (1980) considered cross-flow over a sawtooth shape consisting of six crests and five troughs. More recently unpublished studies examined a single trough imbedded in a flat plain. These two-dimensional models show clearly the recirculation cell that occurs within the basin when a strong inversion caps the basin. As wind speed increases (Froude number increases) the inversion height lowers into the basin and more and more air is flushed out and downwind. Bell and Thompson found that sweeping flows always occurred over the sawtooth land forms when the Froude number exceeded 1.3. Similarly sweeping flows occurred over an isolated basin when the Froude number exceeded 1.2. Cunningham and Bedard (1992) examined the unsteady removal of inversion layers trapped in model mountain valleys. They determined that stagnant air trapped in a mountain basin will first erode, develop a tendency to slosh, develop Kelvin-Helmholtz waves at the interface, and finally fumigate above the upwind face of the basin as winds persist.

2. PHYSICAL MODELING

Simulation of the stably-stratified atmospheric boundary layer interacting with a large open-pit coal mine or mountain basin requires geometric similarity of topographic relief and surface roughness, dynamic similarity of inertial and buoyancy forces, and similarly distributed mean and turbulent upwind velocity and temperature profiles. Viscous and Coriolis forces are not expected to dominate; hence, equivalence of model and prototype Rossby and Reynolds numbers are not required. For these experiments equivalence between approach flow bulk Richardson numbers, $Ri_B = [g(\Delta T/T)\Delta z/(\Delta U)^2]$, and valley Froude numbers, $Fr = [U_h/(gh(T_h - T_o)/T)^{0.5}]$, were sought.

Critical trapping of fumes and combustion products are anticipated to occur during nighttime stable flows; hence, approach flow conditions equivalent to Pasquill categories E and F (Ri_B = 0.014-0.062 and 0.062-0.090 or L_{mo} = 23-125 m and 13-23 m, respectively) are required. It is possible to estimate the near surface temperature gradients required to model E and F stability for different tunnel wind speeds based on Richardson number equality. For a 1:600 scale model a prototype 3.5 ms^{-1} speed at a height of 10 m would require a model wind speed of 0.5 ms^{-1} and a model temperature difference ΔT = 3-13 °C over a 35 mm height for Pasquill Category E conditions and a model temperature difference ΔT = 13-19 °C over the same height for Pasquill Category F conditions.

A range of valley stagnation and partial erosion conditions should occur if model Froude numbers vary between 0.5 to 1.5. Given a 0.5 ms^{-1} model wind speed above a 0.3 m deep model basin, then air temperature differences between the basin bottom and ridge must be $(T_h - T_o)$ = 100°C and 11°C, respectively.

3. EXPERIMENTAL CONFIGURATION

The experiments were to be performed over a large model in the Monash Environmental Wind Tunnel (MEWT: 10 m wide x 7 m high x 40 m long); an inverted model arrangement was chosen; and all heating was provided by electrical resistors placed along a false wind-tunnel roof. A false ceiling 18 m long by 6 m wide was constructed to insert in the MEWT, Figure 2. The ceiling was made modularly from five 3.6 m by 6 m plates and placed 2.5 m above the tunnel floor. In the fourth plate from the entrance a 1:600 generically shaped model basin was constructed to simulate a coal pit or mountain basin. The lower surface of the false roof was covered with aluminum-foil wrapped insulation to reduce heat loss and thermal inertia. All joints between the five plates were taped to smooth intersections and remove leaks.

Heating to produce the stably stratified boundary layer was produced by twenty-four electrical heater elements. Each element was individually rated to 2 kW for a 240 volt potential, but were connected in various serial and parallel combinations. Twelve elements were placed in a vertical grid just downwind of the roof entrance, and twelve more elements were distributed downwind in four rows next to the roof to act as booster heaters. At the low velocities used (0.5 ms^{-1}) dissipation of about 9 kW occurred. This energy sufficed to heat a boundary layer 300 mm thick, which is from five to ten times the depth of the anticipated model-scale Monin-Obukhov stability length, L_{mo} = 30 - 60 mm. Once the wind speed and heater elements were turned on it took from 1 to 2 hours for the flow conditions to stabilize.

Five rows of electrical tape heaters were also adhered to the surface of the model basin as shown in Figure 3. Electrical current to these heaters was adjusted to produce a range of basin surface temperatures. Thus, the approach Richardson number and basin Froude number could be separately adjusted by controlling wind speed, heater element current and heater tape current.

Velocities were measured using a Thermal Systems Inc. Model 1650 temperature corrected hot-film anemometer. Temperatures were measured using an array of ten shielded thermocouple probes. The shielded system was calibrated against aspirated heated air, and the system was found to be accurate within ±0.5°C. Concentrations of helium/air tracer gas mixtures were measured using a mass-spectrometer system. The density of the source gas was adjusted to produce locally neutral buoyancy.

4. FLOW AND CONCENTRATION PATTERNS OVER LARGE BASINS OR MINING PITS

Flow visualization revealed that air flow over the open-pit ranged from fully stagnant situations to complete skimming, Figure 4. Air flow over the inverted surface ranged from fully turbulent to strongly stable. Single traverses of velocity (Figure 5) and temperature (Figure 6) were made nine meters downwind from the wall entrance for a sequence of six different wind speeds ranging from 0.6 to 1.5 ms^{-1}. Examination of semi-logarithmic plots of the velocity distribution reveals that the effective surface drag coefficient and surface roughness for the neutral condition were $u_* / U_{oo} = 0.040$ and $Z_o = 0.020$ mm.

At a Froude number of 0.10-0.55 a strong inversion formed over the basin, wind speeds within the basin were negligible and the basin and boundary layer levels appeared uncoupled. As wind speeds increased (or basin temperatures decreased) the boundary layer penetrated deeper into the basin, and the stagnant layer diminished in depth, Fr = 0.55-0.90. Sometimes the smoke filled mixed layer over the basin appeared to contain Kelvin Helmholtz waves. (Also observed by Cunningham and Bedard, 1992). As the Froude number increased the approach flow penetrated down the side of the upwind basin wall, but then it rose above a stagnant eddy which clung to the downwind region of the basin wall and floor. When conditions permitted the Froude number to increase to 1.3-1.8 the boundary layer fully penetrated the entire basin and flushed all air downstream.

During the first eleven experiments the basin boundary was heated by varying current to the five strip heaters covered by thin metal strips screwed to the bottom of the model basin. Single traverses of temperature were made above the center of the basin for a sequence of seven different wind speeds ranging from 0.1 to 1.45 ms^{-1}, then additional tests were run at a constant wind speed of 0.5 ms^{-1} while the basin surface temperature was reduced by decreasing the strip heater power. Figure 7 displays the temperature profile variation with increased wind speed as Froude number increases from 0.1 to 1.2. Note the progressive penetration of the boundary layer into the basin. A similar temperature profile exists within the basin capped by a strong inversion region. Although Maki and Hariyama (1988) reported a power-law exponent of 1.8 above a quiescent mountain basin; the cross-valley flow situation produces a profile beneath the inversion which falls between curves generated by exponents of 1.8 and 3.0, but does not seem to obey a specific power law.

When the basin surface temperature decreases for constant wind speeds a different set of temperature profiles are produced, Figure 8. In this case the capping inversion decreases rapidly, and the underlying power-law profile region disappears. Smoke released during these runs suggested a wave appears in the boundary flow over the basin, which increases its wavelength and penetrates further into the basin as the basin temperatures decrease (Froude number increases).

a. Isotherm and Streamline Contours

Contour plots were prepared of streamline and temperature cross-sections for both longitudinal and lateral flow sections. Despite the three-dimensional shape of the basin (aspect ratio of $Y/X = 2/3$) streamlines and isotherms were predominately two-dimensional except close to the side walls. Figures 9 displays isotherm (top) and streamline (bottom) contours for an intermediate Froude number of 0.84 Flow penetration observed at the windward edge of the basin during visualization is observed in both isotherm and streamline distributions. The strong inversion appears in the temperature contours as closely spaced isotherms, and the stagnant regions are observed to persist in the downwind portion of the basin by a closed streamline region..

When basin Froude number is less than 0.5 streamfunction and temperature contours above the basin remain nearly horizontal with only a small wave like penetration along the upwind face as warm (cooler in the prototype situation) air drains up into the model basin (downward in the prototype situation). However, when basin Froude number lies between 0.6 to 1.2 the streamline deviations tend to propagate upward (downward in the prototype situation) into the stable capping boundary layer almost undiminished in amplitude. This appears to agree with the projections of linear perturbation theory prepared by Tang (1976) that also predict elevated waves when the product Fr (h/a) is much less than one.

Flow over the center of the basin is definitely two-dimensional despite the fact that the lateral dimension of the basin is only two-thirds the basin length. At smaller basin Froude numbers the planes of constant temperature are essentially horizontal within the basin. Even at larger basin Froude numbers when the boundary layer dips into the basin itself, lateral isotherms are horizontal over the central one-half basin width.

b. Concentration Measurements

Concentrations will increase in the basin after initiation of the source or inception of the inversion condition. Eventually mean concentrations in the open-pit mine will stabilize at their maximum levels. A filling test was performed for stagnation conditions (Fr = 0.62), source located on the downwind face, and sampler located 5 mm above the center of the basin. Concentrations reached a steady value after about 600 seconds, which given a model scale of 1:600 and typical model and field temperatures is equivalent to a prototype time of about 10 hours.

Figure 10 displays concentration contours developed within the basin for up and downwind sources and stagnation for various flow conditions. During stagnation conditions basin concentrations are nearly uniform over the basin height away from the source; whereas upwind basin concentrations are negligible for a downwind source during flushing situations.

Motions within the basin at low basin Froude numbers were too stagnant to be noticeable during smoke visualization. Nonetheless concentration profiles and contours definitely show a preference toward downstream motion for sources released on the upwind face. At larger Froude numbers gases released from the downstream face source only penetrate upwind after extended times. This behavior agrees with the nighttime behavior predicted by linear perturbation theory as developed by Tang (1976).

5. CONCLUSIONS

The intention of this experimental program was to evaluate fumigation and dispersion conditions which might occur within large mountain basins or open-pit mines during stable atmospheric conditions. A novel "upside-down" experimental apparatus was constructed to carry out a measurement program over simulated basins in a large wind tunnel. The general behavior of the flow was found to agree with previous atmospheric experience, salt-water drag tank models, linear perturbation analysis, and computational-fluid-dynamics models.

Acknowledgements

The first author wishes to acknowledge support from the National Science Foundation Cooperative Agreement BCS-882154, CSU/TTU Cooperative Program in Wind Engineering. He also gratefully acknowledges fiscal assistance for lodging and travel provided by the Department of Mechanical Engineering while on study leave at Monash University.

References

Avissar, R., Moran, M.D., Wu, G., Meroney, R.N., and Pielke, R.A.: 1990, "Operating Ranges of Mesoscale Numerical Models and Meteorological Wind Tunnels for the Simulation of Sea and Land Breezes", Boundary-Layer Meteorol., Vol. 50, pp. 227-275.

Beebe, P.S.: 1972, "Turbulent Flow Over a Wavy Boundary," Ph.D. Dissertation, Department of Civil Engineering, Colorado State University, 113 pp. (also THEMIS Technical Report No. 16, June 1972).

Bell, R.C. and Thompson, R.O.R.Y.: 1980, "Valley ventilation by cross winds," J. Fluid Mech., Vol. 96, Part 4, pp. 757-767.

Cermak, J.E.: 1975, "Applications of Fluid Mechanics to Wind Engineering - A Freeman Scholar Lecture", J. Fluids Eng., Vol. 97, pp. 9-38.

Cermak, J.E. and Petersen, R.A.: 1981, "Physical Modeling of downslope mountain wind and atmospheric dispersion," Proc. Fourth U.S. National Conference Wind Engineering Research, Seattle, Washington, 11 pp.

Cunningham, W.J. Jr. and Bedard, A.J. Jr.: 1992, "The Removal of Inversion Layers from Mountain Valleys by an Upper Level Flow: A Scale Model Study," 30th Aerospace Sciences Meeting, January 6-9, 1992, Reno, NV, AIAA paper No. 92-0288, 6 pp.

Davenport, A. and Isyumov, N.: 1967, " The application of the Boundary Layer Wind Tunnel to the prediction of wind loading," Proc. Int. Seminar on Wind Effects on Buildings and Structures, Ottawa, Canada.

Grainger, C. and Meroney, R.N.: 1992, "Dispersion in an Open-Cut Coal Mine in Stably Stratified Flow," Boundary Layer Meteor., (accepted for publication), 31 pp.

Hertig, J.A.: 1986, "Some aspects of exotic simulations," Proceedings Third International Workshop on Wind and Water Tunnel Modelling of Atmospheric Flow and Dispersion, Lausanne, Switzerland, pp. 233-247.

Maki, M., Harimaya, T. and Kikuchi, K.: 1986, "Heat Budget Studies on Nocturnal Cooling in a Basin," J. of Meteorological Society of Japan, Vol. 64, No. 5, pp. 727-740.

Maki, M. and Harimaya, T.: 1988, "The Effect of Advection and Accumulation of Downslope Cold Air on Nocturnal Cooling in Basins," J. of Meteorological Society of Japan, Vol. 66, No. 8, pp. 581-597.

Melbourne, W.H.: 1977, "Development of Natural Wind Models at Monash University," 6th Aust. Hydraulics and Fluid Mechanics Conference, Adelaide, pp. 190-194.

Meroney, R.N.: 1981, "Physical simulation of dispersion in complex terrain and valley drainage flow situations", Air Pollution Modeling and Its Application, Ed. C. De Wispelaere, Plenum Publishing Co., 21 pp.

Meroney, R.N.: 1987, "Guidelines for Fluid Modeling of Dense Gas Cloud Dispersion", Journal of Hazardous Materials, Vol. 17, pp. 23-46.

Meroney, R.N.: 1990, "Fluid Dynamics of Flow over Hills/Mountains--Insights Obtained through Physical Modeling", Chapter 7 of Atmospheric Processes Over Complex Terrain, Ed. W. Blumen, American Meteorological Society Monograph No. 45, pp. 145-171.

Meroney, R.N., Cermak, J.E. and Yang, B.T.: 1975, " Modeling of Atmospheric Transport and Fumigation at Shoreline Sites", Boundary-Layer Meteorol., Vol. 9, pp. 69-90.

Tang, W.: 1976, "Theoretical Study of Cross-Valley Wind Circulation," Arch. Met. Geoph. Biokl., Ser. A, Vol. 25, pp. 1-18.

Snyder, W.H.: 1972, "Similarity Criteria for the Application of Fluid Models to the Study of Air Pollution Meteorology", Boundary-Layer Meteorol., Vol. 3, pp. 113-134.

Whiteman, C.D.: 1990, "Mountain Meteorology," Chapter 1 from Atmospheric Processes Over Complex Terrain, American Meteorological Society Monograph Vol. 23, No. 45, pp. 1-42.

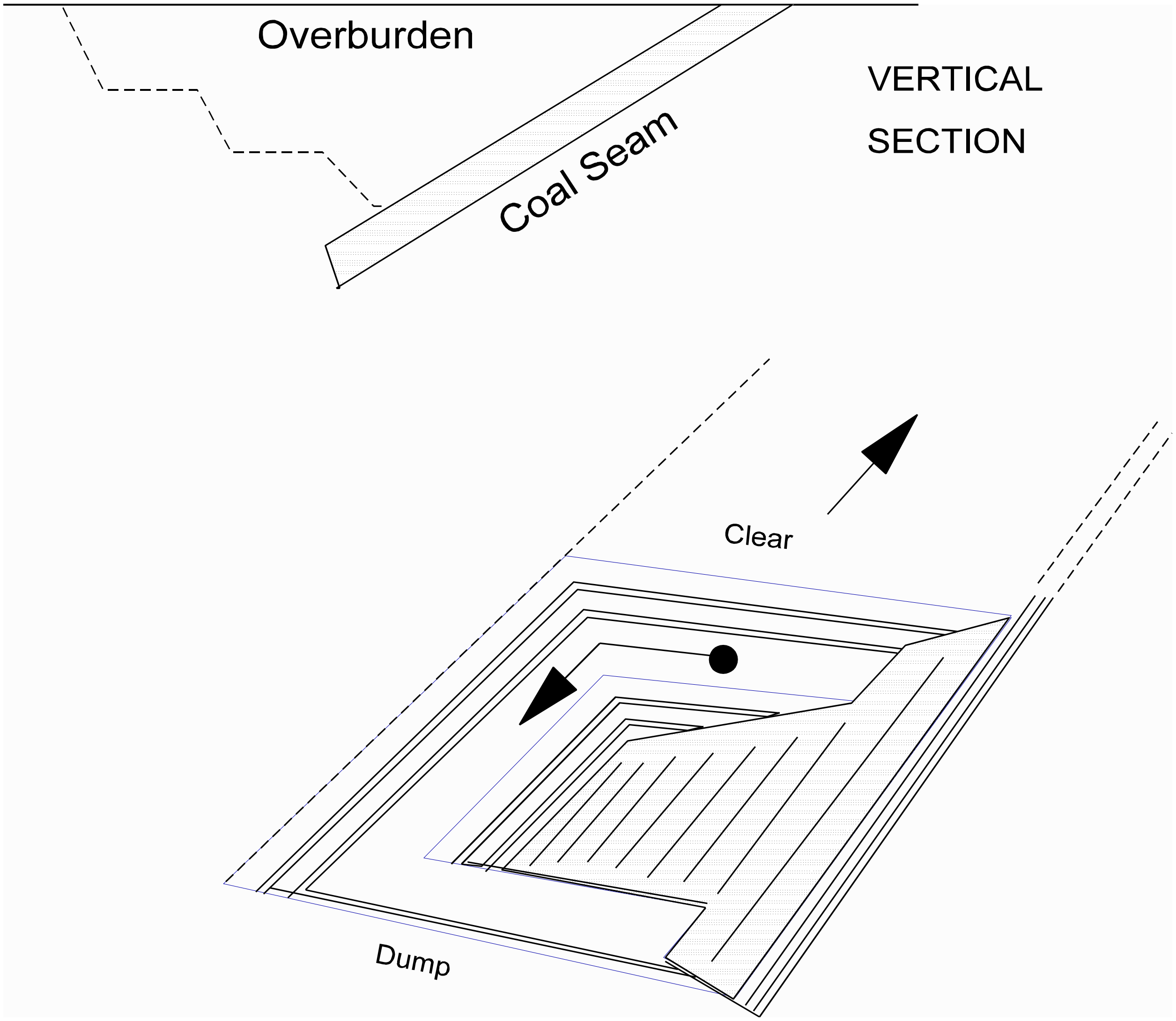

Fig. 1 Schematic of typical terrace-type open-pit coal mine. Typical dimensions: 1800 m long, 1000 m wide and 200 m deep.

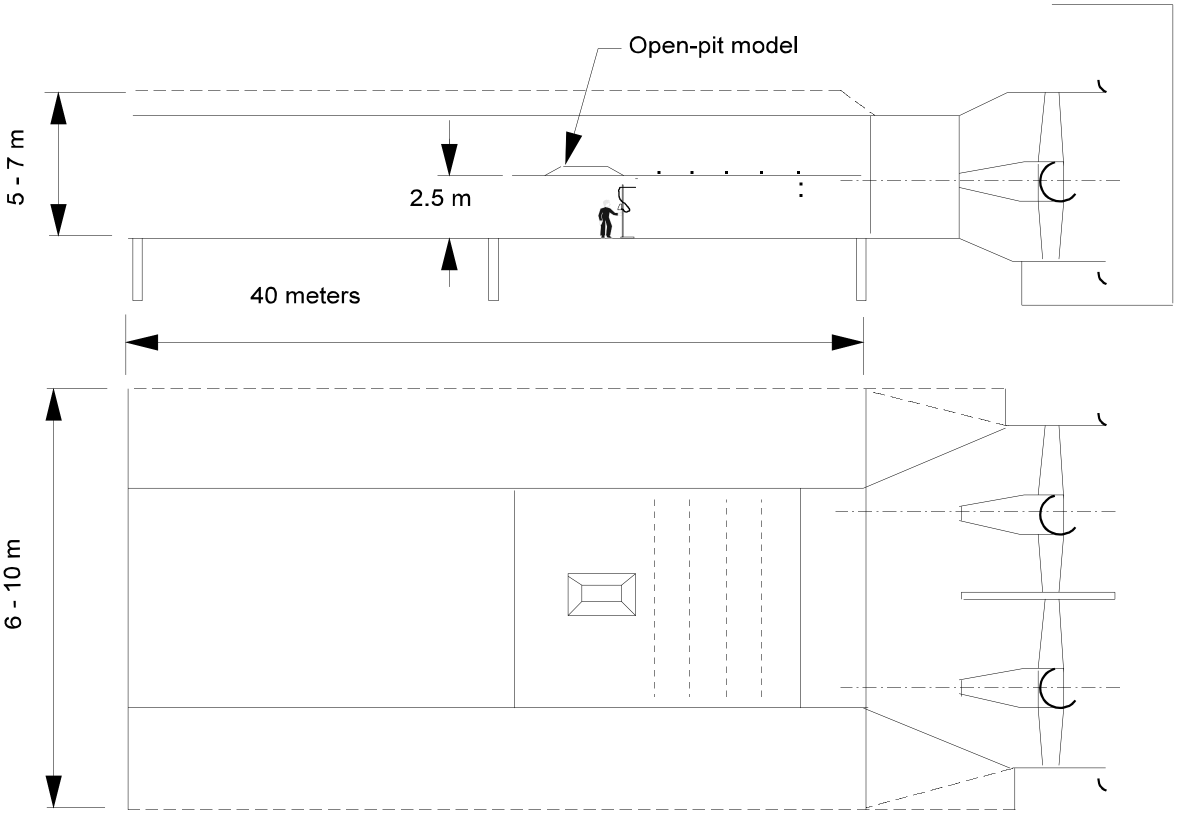

Fig. 2 Inverted open-pit mine or mountain basin model installed in Monash Environmental Wind Tunnel. All tests performed on lower false roof surface.

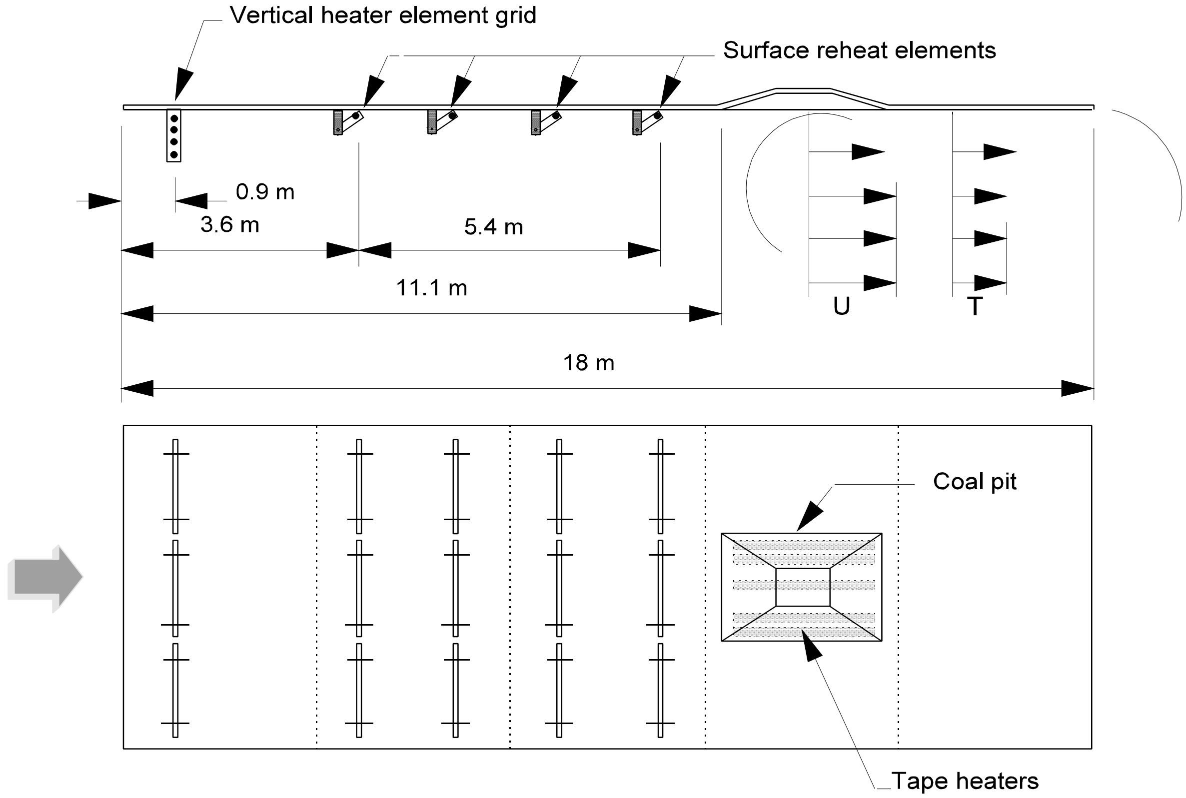

Fig. 3 Inverted-model open-pit coal mine or mountain basin configuration for insertion in the Monash Environmental Wind Tunnel. Twenty-four heater elements are each 2 m long @ 29 ohms or 2 kW capacity.

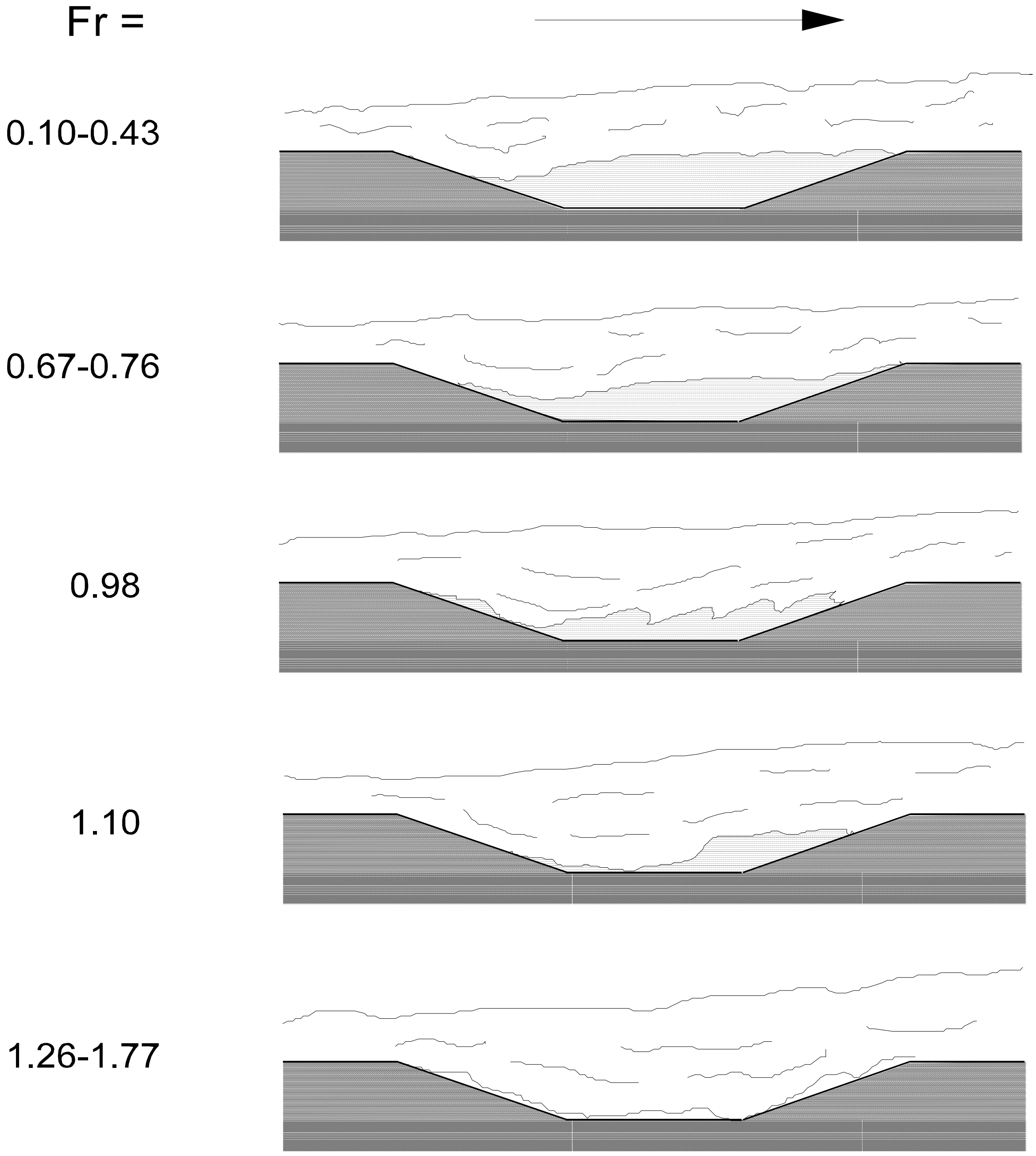

Fig. 4 Smoke appearance during sequence of visualizations of flow over model basin. As wind-tunnel speed increases from 0.1 to 1.45 ms^{-1} pit Froude number varies from 0.1 to 1.77.

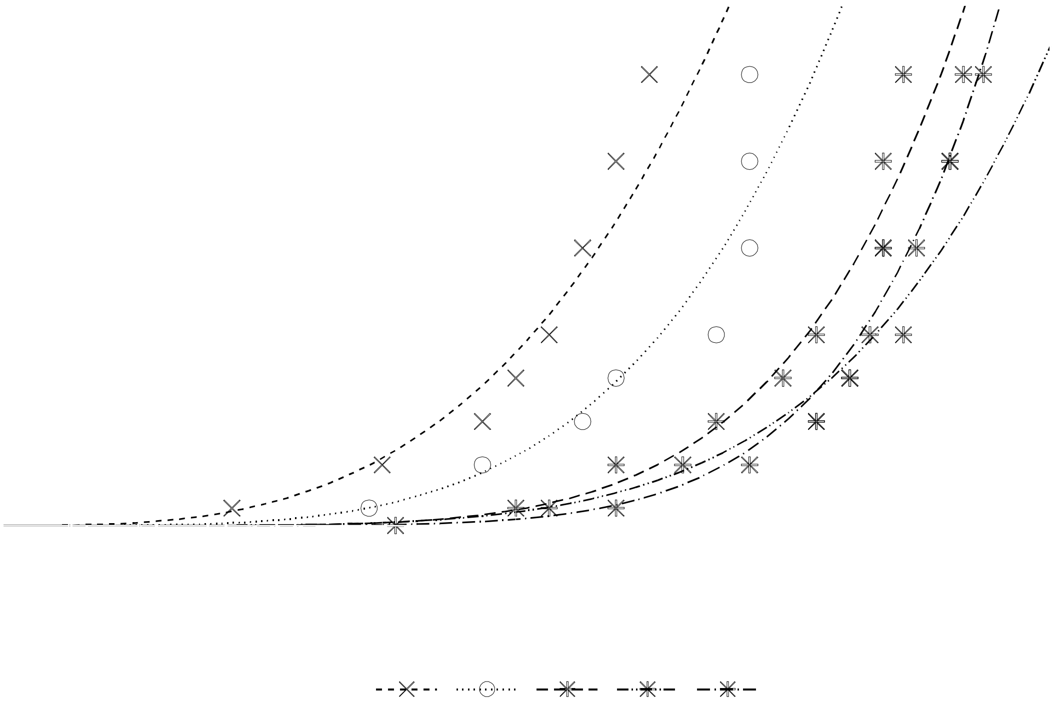

Fig. 5 Velocity profiles measured beneath inverted floor system for stably stratified flows in Monash Environmental Wind Tunnel.

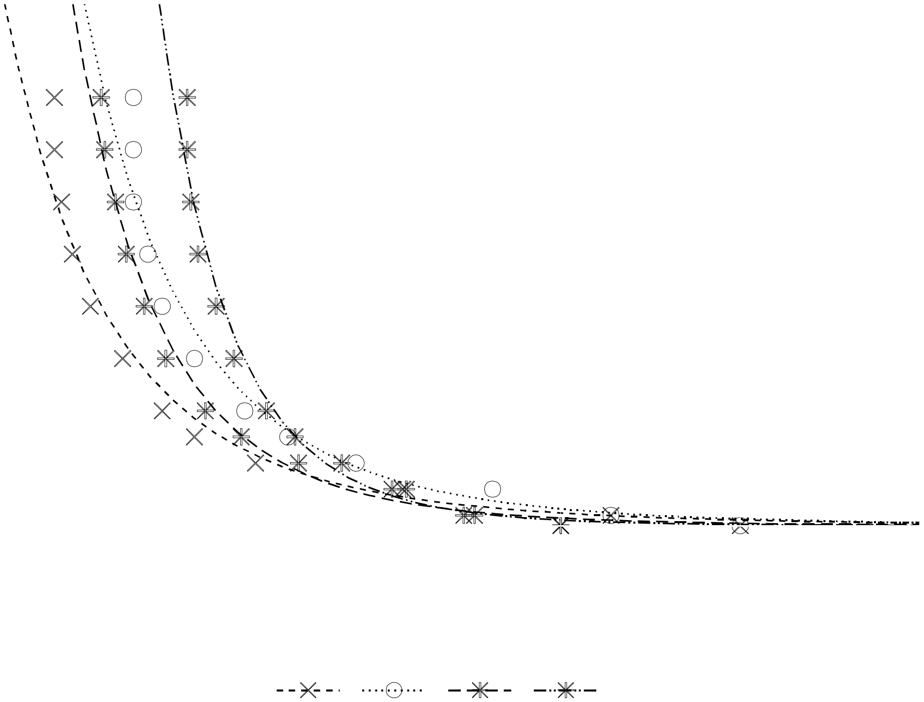

Fig. 6 Temperature profiles measured beneath inverted floor system for stably stratified flows in Monash Environmental Wind Tunnel.

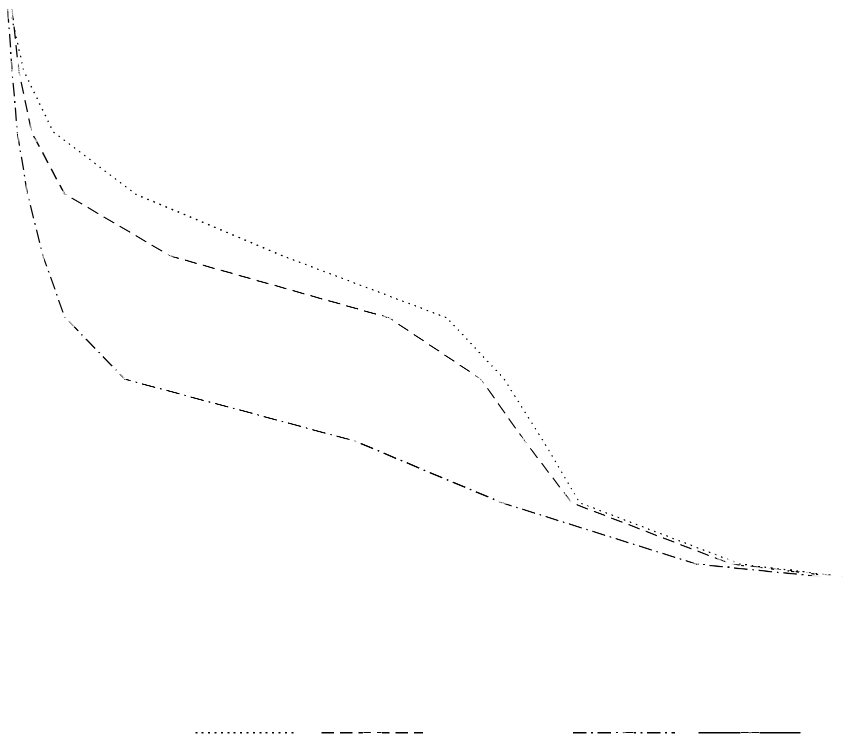

Fig. 7 Vertical profiles above center of model basin. As velocity increases from 0.10 to 1.45 ms^{-1} the basin Froude number varies from 0.10 to 1.28.

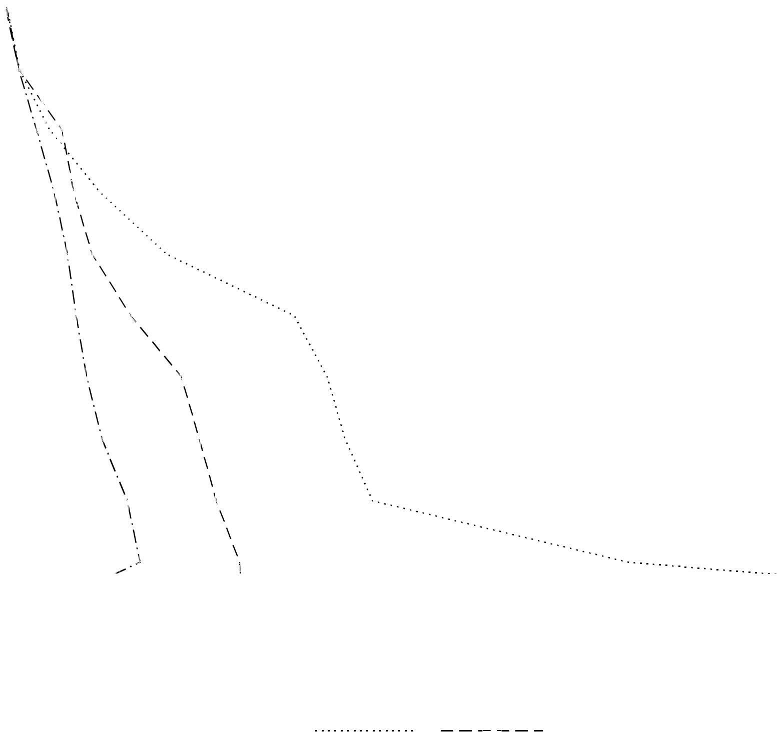

Fig. 8 Temperature profiles over center of basin model for constant wind speed and variable basin surface temperature. As basin temperature decreases from 186°C to 50°C the basin Froude number varies from 0.38 to 1.26.

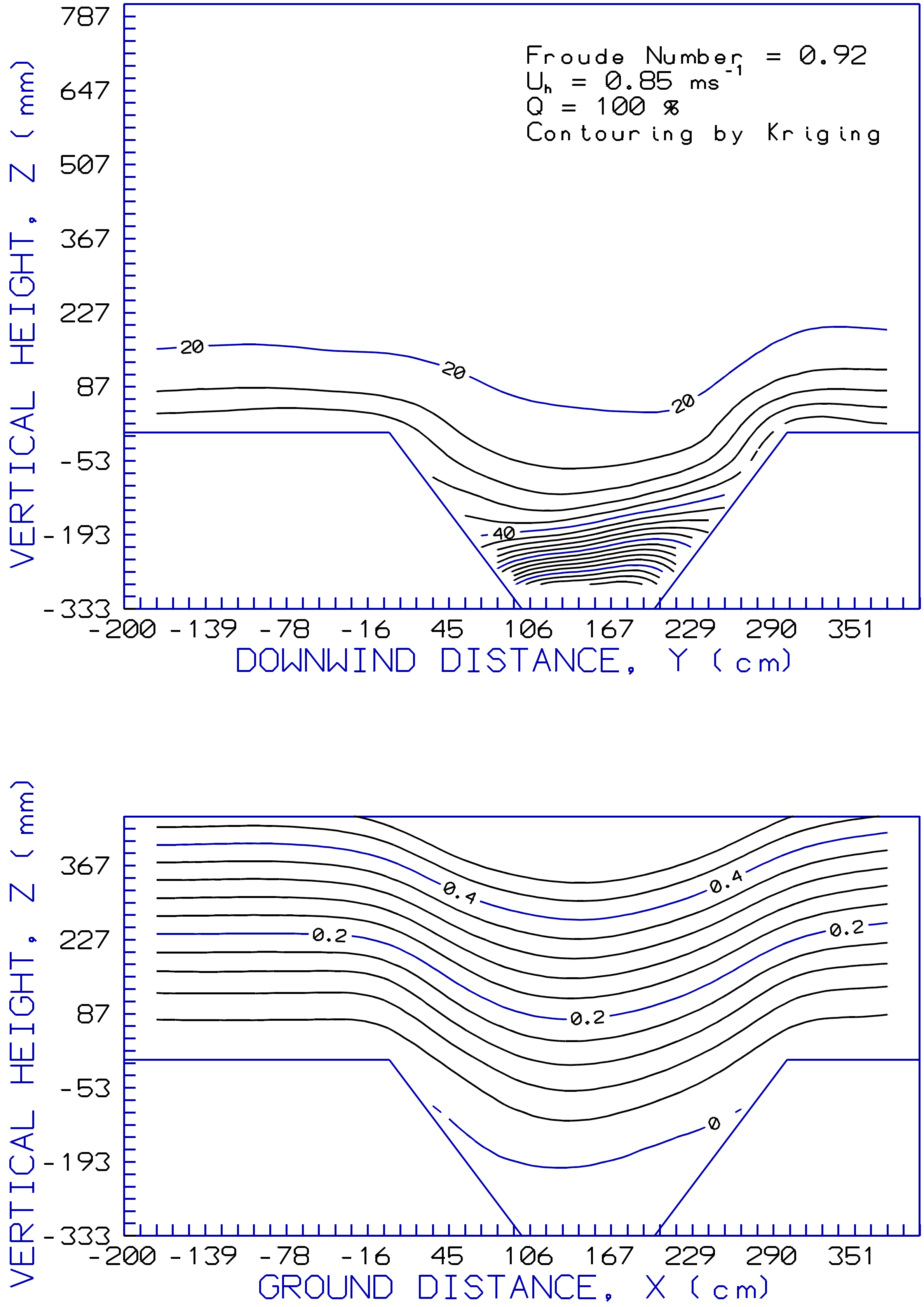

Fig. 9 Isotherms (ºC) and streamline (m^2/s) contours over basin model. Fr = 0.92.

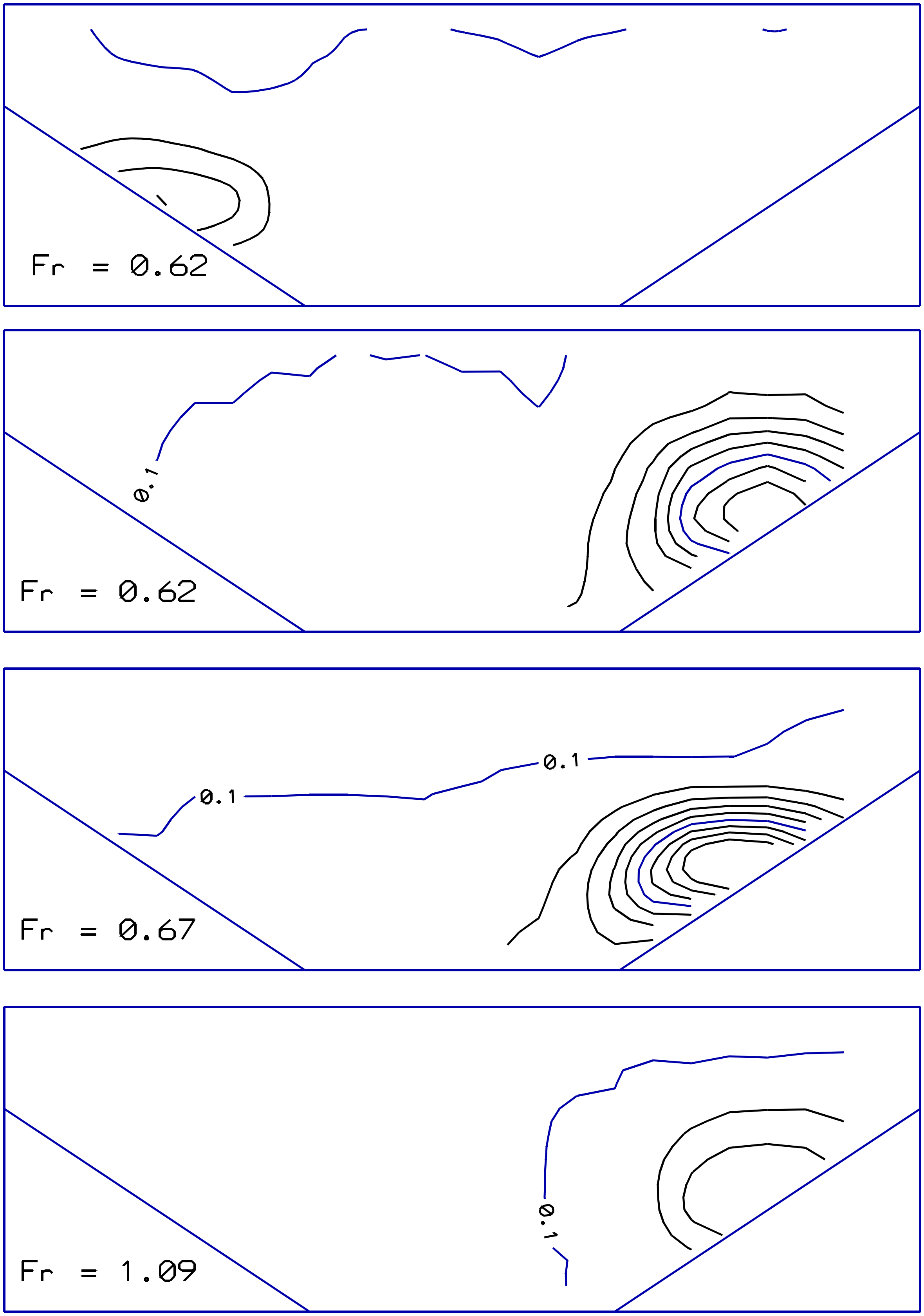

Fig. 10 Contours of concentration (ppt) for various release configurations.